Space Shift Keying Modulation for MIMO Channels

Jeyadeepan Jeganathan, Ali Ghrayeb, *Senior Member, IEEE,* Leszek Szczecinski, *Senior Member, IEEE,* and Andres Ceron

***Abstract*—In this paper, we present space shift keying (SSK) as a new modulation scheme, which is based on spatial modulation (SM) concepts. Fading is exploited for multiple-input multiple-output (MIMO) channels to provide better performance over conventional amplitude/phase modulation (APM) techniques. In SSK, it is the antenna index used during transmission that relays information, rather than the transmitted symbols themselves. This absence of symbol information eliminates the transceiver elements necessary for APM transmission and detection (such as coherent detectors). As well, the simplicity involved in modulation reduces the detection complexity compared to that of SM, while achieving almost identical performance gains. Throughout the paper, we illustrate SSK's strength by studying its interaction with the fading channel. We obtain tight upper bounds on bit error probability, and discuss SSK's performance under some non-ideal channel conditions (estimation error and spatial correlation). Analytical and simulation results show performance gains over APM systems (3 dB at a bit error rate of 10^{-5}), making SSK an interesting candidate for future wireless applications. We then extend SSK concepts to incorporate channel coding, where in particular, we consider a bit interleaved coded modulation (BICM) system using iterative decoding for both convolutional and turbo codes. Capacity results are derived, and improvements over APM are illustrated (up to 1 bits/s/Hz), with performance gains of up to 5 dB.**

***Index Terms*—Multiple antenna array, spatial modulation.**

I. Introduction

MULTIPLE antennas in wireless systems offer a practical way to extend next generation communication capabilities. Their unprecedented improvements over single antenna systems have spawn a wealth of research in multiple-input multiple-output (MIMO) communications, which fall under three general themes.

The first is spatial multiplexing: exploiting multiple antennas to transmit more information. One example is the vertical Bell Laboratories layered space-time (V-BLAST) architecture [1], where an array of symbols are layered in space, and transmitted simultaneously over all antennas. Spatial multiplexing requires synchronizing all antennas to transmit at the same time, and introduces interference from all antennas during reception, making for complex detection schemes. Practical integration of V-BLAST for example, requires sub-optimal, low complexity receivers [2]. For adequate performance, in most cases, these receivers require the number of receive antennas to be larger or equal to the number of transmit antennas, which is not practical for downlink transmission to small mobile devices.

The next type of MIMO system is diversity transmission. In this case, antennas are used to increase the reliability of the message. Similar to channel coding, diversity systems exploit the spatial domain as a coding mechanism to increase reliability (i.e., diversity). These types of systems also requires synchronizing all antennas to transmit at the same time. The first form of spatial diversity (applicable for two transmit antennas) is the Alamouti scheme [3], which achieves transmit diversity. However, this diversity is attained at the expense of transmission rate, which remains unchanged from a single-input multiple-output (SIMO) system.[1] As opposed to spatial multiplexing, diversity schemes provide simpler detection due to certain transmission properties. For example, orthogonal space time block codes (OSTBCs), such as the Alamouti scheme, circumvent the interference caused by transmitting on multiple antennas due to the orthogonality of the codebook. However, higher transmit diversity is only achieved at the expense of transmission rate, since full-rate OSTBCs only exist for two transmit antennas (complex constellations), and eight or less transmit antennas (real constellations) [4].

Finally, the third category is hybrid transmission: both spatial multiplexing and diversity concepts are integrated. The first application of hybrid transmission is multilayered space-time coding, introduced by Tarokh et al. in [5], which exploits transmit antennas to increase both diversity and transmission rate. However, these benefits are achieved at the expense of increased detection complexity.

All of these systems provide their own sets of benefits and restraints, but are flexible enough to accommodate various requirements. However, some common pitfalls amongst MIMO systems are:

1) Inter-channel interference (ICI): Introduced by coupling multiple symbols in time and space.
2) Inter-antenna synchronization (IAS): In the BLAST and OSTBC architectures, the detection algorithms assume

Manuscript received July 8, 2008; revised November 8, 2008; accepted January 17, 2009. The associate editor coordinating the review of this paper and approving it for publication was G. Colavolpe.

J. Jeganathan was with the ECE Department at Concordia University, Montreal, Canada. He is now with Ericsson, Montreal, Canada (jeyadeepan.jeganathan@ericsson.com).

A. Ghrayeb is with the ECE Department at Concordia University, Montreal, Canada (aghrayeb@ece.concordia.ca).

L. Szczecinski is with INRS-EMT at the University of Quebec, Montreal, Canada (leszek@emt.inrs.ca).

A. Ceron is with the Department of Electronics Engineering, Universidad Técnica Federico Santa Maria, Avenida Espana 1680, Valparaíso, Chile (corales@emt.inrs.ca).

This work was supported in part by NSERC (Canada), under a Post Graduate Scholarship (PGS) and by FQRNT (Quebec), under research grant F00803.

Digital Object Identifier 10.1109/TWC.2009.080910

[1]Rate refers to the number of information bits/s/Hz.

that all symbols are transmitted at the same time. Hence, IAS is necessary to avoid performance degradation [6], consequently increasing transmitter overhead. For example, Agilent Technologies' signal studio for 3GPP W-CDMA HSPA [7] needs to automatically configure the input and output synchronizing trigger signal when transmit diversity antennas are selected.

3) Radio frequency (RF) chains: Although multiple antenna elements are relatively inexpensive to deploy, and the digital signal processing requirements are feasible due to increased industry growth, the necessary RF elements are not as simple to implement [8]. These RF chains are bulky, expensive, and necessary for each antenna that is used. One feasible method around the problem is to employ antenna selection (AS) [8]–[12] (and references therein).

   In order to exploit MIMO benefits however, there is a limit to the amount of reductions in RF chains offered by AS methods. Most of the advantages obtained through MIMO communications is due to multiple *transmit* antennas. For example, in V-BLAST, multiple transmit antennas increase the spectral efficiency of the system without additional bandwidth requirement (compared to that of a SIMO system). For diversity systems, such as OSTBCs, it is multiple transmit antennas that significantly increase the system's diversity. So, although AS provides some reduction in RF chains, there is no way around avoiding the increase in RF chains compared to that of a single antenna system. As well, AS generally increases the overhead at the receiver, and is prone to feed back errors in the case of transmit AS.

In this paper, we target these problems by developing space shift keying (SSK) modulation for MIMO channels, which considers an alternate method for transmitting information. Before continuing however, we first elaborate on some important previous work that gave rise to the idea of SSK modulation.

A. Prior Work

Spatial Modulation (SM): The underlying idea of SM introduced by Mesleh et al. in [13], is actually conceptualized earlier (to some extent) by Chau et al. in [14][15]. In [14], a scheme entitled SSK is proposed, in which *distinct* multipath characteristics from different antennas are used to discriminate between transmitted symbols.[2] The receiver determines which mode of transmission is used (either one antenna or both antennas are activated) in order to detect the message. Chau et al. also mention extensions of their binary scheme to higher order modulation by combining amplitude/phase modulation (APM), which is similar in concept to SM. However, they only consider the case of two transmit antennas, and their scheme does not avoid ICI and IAS.

Exploiting antenna indices as a source of information is also covered in [6], [16], where precoded sequences of symbols are transmitted using only one antenna. The symbol, in conjunction with the antenna index, is used to decode the message. However, these schemes suffer from lower spectral efficiency due to the employment of parity symbols. Also, only the case of binary/quadrature phase shift keying (BPSK/QPSK) are considered. To overcome the problem of spectral efficiency loss, and in order to generalize to other modulation schemes, SM is introduced. SM is a pragmatic approach for transmitting information, where the modulator uses well known APM techniques, such as quadrature amplitude modulation (QAM), but also employs the antenna index to convey information. SM is then extended to OFDM in [17], and its performance under non-ideal channel conditions (spatial correlation, mutual antenna coupling) is analyzed in [18]. We note that the SM detector in [13] is based on an ad hoc design, and only functions under some artificial assumptions about the channel (see [19] for details). On the other hand, SM optimal detection (SM-OD) under conventional channel assumptions is derived in [19], and shown to outperform V-BLAST and MRC schemes ($1.5 - 3$ dB at a bit error rate of 10^{-5}).

SSK versus SM: In SSK, antenna indices are used as the *only* means to relay information, which makes it somewhat a special case of SM. However, this elimination of APM provides SSK with notable differences and advantages over SM:

1) Detection complexity is lowered, while the performance is almost identical to SM-OD.
2) Because phase and amplitude of the pulse do not convey information, transceiver requirements are less stringent than for APM (e.g., non-coherent detectors may be considered).
3) The simplicity of SSK's framework provides ease of integration within communication systems. For example, one envisioned application is ultra wide band (UWB), where it is pulses that are used rather than APM signals.

All of this, as well as SM's inherent advantages, motivates our presentation of the SSK modulation technique.

B. Contribution

Concepts: We present the SSK modulation technique, in which the spatial domain is solely exploited to convey information. All of the aforementioned advantages comprising SM are present, while providing reductions in transmitter overhead and detection complexity. The constellation space is analyzed to illustrate the source of SSK's strengths over APM schemes. This analysis allows for a strong foundation in understanding SM parameters that may be chosen to obtain better performance gains (SM trade-offs between the number of transmit antennas and the APM constellation size is chosen heuristically in [20]). Extensions to incorporate practical coding schemes are also presented. In particular, we present a bit interleaved coded modulation (BICM) system using iterative decoding, where both convolutional and turbo coded modulation (CM) are employed.

Analysis: Tight upper bounds on performance are derived. For the uncoded case, upper bounds on bit error rate (BER) are obtained using union bounding techniques, and nearest neighbor analysis. The diversity of the system is also shown.

[2]We note that SSK in [14] and in this paper have *different* meanings. We use the same name because SSK is truly descriptive of the scheme we develop later in Section II.

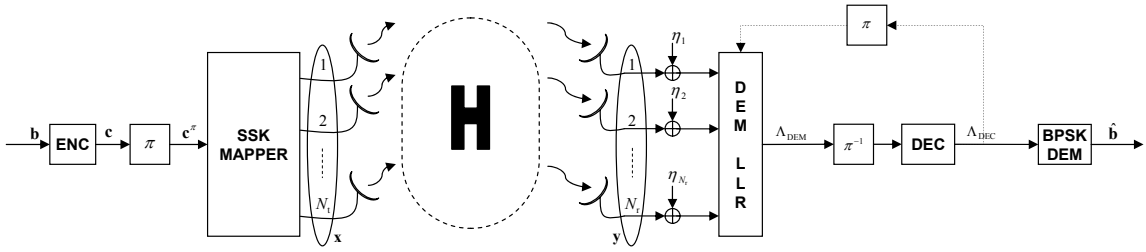

Fig. 1. SSK system model.

CM performance is analyzed using saddlepoint approximation techniques, and upper bounds on BICM BER are obtained for fast fading channels. Capacity results are also obtained, demonstrating spectral efficiency gains over APM-CM techniques.

Results: Extensive simulations are provided to support our analysis, and illustrate SSK's potential for integration in future wireless systems. We also compare SSK's performance with SM, V-BLAST, and single antenna APM techniques, for various antenna and channel conditions.

C. Organization

Section II introduces the basic system model, including the mapping and detection process, in which we also give a detailed analysis of SSK's constellation space. In Section III, we present analytical results on the bit error probability, as well as a complexity comparison with other systems. We discuss the coded SSK system in Section IV, where we present capacity and analytical performance results. Section V provides thorough simulation results on performance, and we conclude the paper in Section VI.

D. Notation

Italicized symbols denote scalar values, while bold lower/upper case symbols denote vectors/matrices. We use $(\cdot)^T$ for transpose, $(\cdot)^*$ for complex conjugate, $(\cdot)^H$ for conjugate transpose, $\binom{\cdot}{\cdot}$ for the binomial coefficient, and $\|\cdot\|_{\mathrm{F}}$ for the Frobenius norm of a vector/matrix. We use $\mathcal{CN}\left(\mathfrak{m}, \sigma^2\right)$ for the complex Gaussian distribution of a random variable, having independent Gaussian distributed real and imaginary parts denoted by $\mathcal{N}\left(\mathfrak{m}, \frac{\sigma^2}{2}\right)$, with mean $\mathfrak{m}$ and variance $\frac{\sigma^2}{2}$. We use $P(\cdot)$ for the probability of an event, $p_{\mathbf{Y}}(\cdot)$ for the probability density function (PDF) of a random variable $\mathbf{Y}$, and $E_{\mathbf{x}}[\cdot]$ for the statistical expectation with respect to $\mathbf{x}$. We use $\log(\cdot)$ for the natural logarithm (i.e. base e), and $\log_a(\cdot)$ for the logarithm with base a. We use $\mathrm{Re}\{\cdot\}$ for the real part of a complex variable, $\mathcal{X}$ to represent a constellation of size M, and $\mathcal{X}_c^k$ to denote a subset of $\mathcal{X}$ containing all constellation points with the k^{th} bit equal to $c \in \{0, 1\}$.

II. SSK Modulation

The general system model consists of a MIMO wireless link with N_{t} transmit and N_{r} receive antennas, which is illustrated in Fig. 1. A random sequence of independent bits $\mathbf{b} = \begin{bmatrix} b_1 & b_2 & \cdots & b_k \end{bmatrix}$ enter a channel encoder with output $\mathbf{c} = \begin{bmatrix} c_1 & c_2 & \cdots & c_n \end{bmatrix}$, where k and n represent the number of encoder inputs and outputs, respectively. The pseudo randomly interleaved sequence $\mathbf{c}^{\pi}$ then enters an SSK mapper, where groups of $m = \log_2(N_{\mathrm{t}})$ bits are mapped to a constellation vector $\mathbf{x} = \begin{bmatrix} x_1 & x_2 & \cdots & x_{N_{\mathrm{t}}} \end{bmatrix}^T$, with a power constraint of unity (i.e. $E_{\mathbf{x}}\left[\mathbf{x}^H\mathbf{x}\right] = 1$). In SSK, one antenna remains active during transmission and hence (ideally), only one RF chain is required. However, due to pulse shaping, the transmitted pulse will extend a few symbol periods, and restrict the RF chain from being switched to another antenna.[3] In the UWB framework however, the cost of RF chains is fixed regardless of the number of antennas since pulse shaping is not required. The discussion in this paper may be extended to UWB indoor communications using the appropriate statistical channel models given in [21].

The modulated signal is then transmitted over an $N_{\mathrm{r}} \times N_{\mathrm{t}}$ wireless channel $\mathbf{H}$, and experiences an $N_{\mathrm{r}} - \dim$ additive white Gaussian (AWGN) noise $\eta = \begin{bmatrix} \eta_1 & \eta_2 & \cdots & \eta_{N_{\mathrm{r}}} \end{bmatrix}^T$. The received signal is given by $\mathbf{y} = \sqrt{\rho}\mathbf{H}\mathbf{x} + \eta$, where ρ is the average signal to noise ratio (SNR) at each receive antenna, and $\mathbf{H}$ and η have independent and identically distributed (iid) entries according to $\mathcal{CN}(0, 1)$.

At the receiver side, the SSK detector estimates the antenna index that is used during transmission, and demaps the symbol to its component bits $\hat{\mathbf{b}}$.

A. Transmission

SSK modulation consists of groups of m bits that are mapped to a symbol x_j, which is then transmitted from the j^{th} antenna. We note that, although the symbol itself does not contain information, it might be designed to optimize transmission. For now, we use $x_j = 1$ for all j, and refer the reader to [22] for optimized symbol transmission. Even though x_j does not convey information, its location in $\mathbf{x}$ does. The vector $\mathbf{x}$ specifies the activated antenna, during which all other antennas remain idle, and has the following form:

$$\mathbf{x}_j \triangleq \begin{bmatrix} 0 & 0 & \cdots & \underset{\substack{\uparrow \\ j^{\text{th}} \text{ position}}}{1} & 0 & \cdots & 0 \end{bmatrix}^T.$$

[3]Therefore, at the most, we would require the number of RF chains to equal the number of symbol period durations in the transmitted pulse.

Hence, the channel output is given by $\mathbf{y} = \sqrt{\rho}\mathbf{h}_j + \eta$ when the j^{th} antenna is used, where

$$\mathbf{h}_j \triangleq j^{\text{th}} \text{ column of } \mathbf{H}.$$

Remark 1: Only one column of $\mathbf{H}$ (i.e., $\mathbf{h}_j$) is *activated*, and the column changes depending on the transmitted symbol. Essentially, these columns act as *random* constellation points for SSK modulation.

An example of SSK modulation for 2 bits/s/Hz transmission is given in Table I. In general, M-ary SSK modulation (i.e., where $\log_2(M)$ bits are transmitted per channel use) requires N_{t} to equal M. In cases where this N_{t} requirement is difficult to meet (ex., due to hardware constraints), generalized SSK (GSSK) may be employed (see [23] for details).

TABLE I
EXAMPLE OF THE SSK MAPPER RULE.

$\mathbf{b} = [b_1 \quad b_2]$	symbol	antenna index j	$\mathbf{x} = [x_1 \quad \cdots \quad x_4]^T$
$[0 \quad 0]$	0	1	$[1 \quad 0 \quad 0 \quad 0]^T$
$[0 \quad 1]$	1	2	$[0 \quad 1 \quad 0 \quad 0]^T$
$[1 \quad 0]$	2	3	$[0 \quad 0 \quad 1 \quad 0]^T$
$[1 \quad 1]$	3	4	$[0 \quad 0 \quad 0 \quad 1]^T$

B. Detection

In the uncoded case, the detector's main function is to determine the antenna index used at the transmitter. Coded detection will be discussed in Section IV-C. Since the channel inputs are assumed equally likely, the optimal detector is maximum likelihood (ML), which is given by

$$\begin{aligned}\hat{j} &= \arg\max_j p_{\mathbf{Y}}(\mathbf{y} \mid \mathbf{x}_j, \mathbf{H}) = \arg\min_j \|\mathbf{y} - \sqrt{\rho}\mathbf{h}_j\|_{\text{F}}^2 \\ &= \arg\max_j \text{Re}\left\{\left(\mathbf{y} - \tfrac{\sqrt{\rho}}{2}\mathbf{h}_j\right)^H \mathbf{h}_j\right\}, \end{aligned} \quad (1)$$

where $\hat{j}$ represents the estimated antenna index, $1 \le j \le N_{\text{t}}$, and $p_{\mathbf{Y}}(\mathbf{y} \mid \mathbf{x}_j, \mathbf{H})$ is given by

$$p_{\mathbf{Y}}(\mathbf{y} \mid \mathbf{x}_j, \mathbf{H}) = \frac{\exp\left(-\left\|\mathbf{y} - \sqrt{\rho}\mathbf{H}\mathbf{x}_j\right\|_{\text{F}}^2\right)}{\pi^{N_{\text{r}}}}. \quad (2)$$

C. Constellation

To analyze SSK's constellation, we first consider a fixed channel realization $\mathbf{H}$, and the effective $N_{\text{r}} - \dim$ constellation symbol $\mathbf{x}_{j,\text{eff}}$ that results from the following channel transformation:

$$\mathbf{x}_{j,\text{eff}} = \mathbf{H}\mathbf{x}_j. \quad (3)$$

These effective constellation points are shown in Fig. 2 for both APM and SSK. In APM, the effective constellation $\mathcal{X}^{\text{eff}}$ is composed of scaled versions of the vector $\mathbf{h}x_j$.[4] However, SSK's $\mathcal{X}^{\text{eff}}$ is made up of scaled versions of *all* columns of $\mathbf{H}$. That is, in terms of the constellation points, x_j is fixed while $\mathbf{h}_j$ changes in SSK, whereas x_j changes while $\mathbf{h}_j$ is fixed in APM. Decisions for APM are performed in the $1 - \dim$ complex space, independent of which antenna is used (i.e., after matched filtering, the sufficient statistics are scalar). On the other hand, SSK decisions are made in the $N_{\text{r}} - \dim$ space.

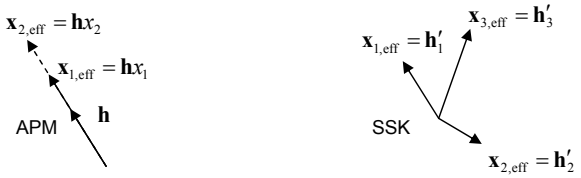

Fig. 2. Illustration of the effective constellation space $\mathcal{X}^{\text{eff}}$.

From these observations, it is clear that we expect SSK to outperform APM schemes for increasing M and N_{r}. As well, superior performance can be achieved for channel realizations $\mathbf{H}$ having columns that are widely spread apart in the $N_{\text{r}} - \dim$ space. This of course depends on the stochastic properties of the channel, and can be exploited in adaptive transceiver schemes (see [22] for details).

We note that, it is using the antenna index as the source of information that increases the size of the constellation space, and *not* the fact that different antennas are being used for transmission. For example, if APM with transmission on alternating antenna indices is considered, $\mathcal{X}^{\text{eff}}$ would not change since, at any given time, the receiver explores only all possible transmit *symbols*. The actual *antenna index* is assumed to be known at the receiver, and remains the same regardless of the transmitted symbol. If, on the other hand, both the antenna index and the transmit symbol convey information, the modulation scheme is no longer APM, but rather SM. In this case, $\mathcal{X}^{\text{eff}}$ is similar to SSK, but with the possibility of having more than one scaled version of $\mathbf{x}_{j,\text{eff}}$ along the same direction in Fig. 2 (since both x_j and $\mathbf{h}_j$ are changing).

D. Practical Issues

Before proceeding further, we present a discussion on SSK's feasibility in real world wireless systems. In this section, we discuss two main concerns with SSK modulation, namely hardware requirements and antenna switching, as well as methods to overcome these problems.

Hardware Requirements: The number of transmitting antennas required is an apparent drawback of the scheme, since N_{t} can grow quite large for high data rates. Therefore, it is impractical to implement on small mobile stations, but can be used for downlink base station transmission, where the available resources for antenna deployment is more flexible. Still, there is a limit to this flexibility, and in such cases, GSSK is a viable solution. GSSK, a variant SSK scheme presented in [23], makes it possible to reduce the requirement on the number of transmit antennas at the expense of performance. The basic concept of GSSK is to use *combinations* of antenna indices to transmit information, rather than only one index (as in SSK). The combination of SSK and GSSK allows

[4]The subscript j is absent in $\mathbf{h}$ to denote that for APM, the antenna does not change, and even if it did, it does not contribute in any information about the transmitted message.

for a strong foundation in building practical systems, and provides enough flexibility to accommodate different hardware constraints.

Regardless of employing GSSK, or restricting SSK modulation to downlink transmission, the overhead in transmit antennas will be more than conventional MIMO wireless techniques, such as V-BLAST for example. However, we note that one important difference between the two is that SSK requires only one RF chain (ideally). The major bottleneck of implementing multiple antennas (i.e., bulky RF chains) is hence reduced, at the expense of increasing antenna elements. The actual benefits of this hardware reduction for practical integration purposes are difficult to evaluate at this point and require further investigation, but the potential for the complexity-perfomance trade-off is clearly present.

Antenna Switching: To transmit information in SSK, the antenna index needs to vary, and will constantly remain in a switching state. However, due to pulse shaping, the transmitted pulse will extend a few symbol periods and restrict the RF chain from being switched to another antenna. We would then, at the most, require the number of RF chains to equal the number of symbol period durations in the transmitted pulse. Therefore, more than one RF chain might be necessary. For the UWB framework on the other hand, the cost of RF chains remains fixed since pulse shaping is not required (i.e., only one RF chain is needed regardless of N_{t}). Hence, extensions of SSK to UWB communications is an interesting topic, and is possible using the appropriate statistical channel models given in [21]. For example, one possible channel model is the Nakagami distribution, which is shown to simulate small scale fading amplitudes in UWB indoor systems.

Given the aforementioned discussion, SSK's integration into current wireless systems is a topic worthwhile investigating, and is done so in detail within the next few sections.

III. Performance Analysis

In this section, we present analytical results on SSK's uncoded performance. A tight upper bound on the bit error probability is derived, and we explicitly determine SSK's diversity order.

A. Uncoded Error Probability

SSK's performance is derived using the well known union bounding technique [24, p. 261-262]. The average BER for SSK is union bounded as

$$\begin{aligned} P_{\mathrm{e,bit}}^{\mathrm{SSK}} &= E_j\left[\bigcup_{\hat{\jmath},\hat{\jmath}\neq j} N(j,\hat{\jmath})P\left(\mathbf{x}_j \to \mathbf{x}_{\hat{\jmath}}\right)\right] \\ &\leq \sum_{j=1}^{N_{\mathrm{t}}}\sum_{\hat{\jmath}=j+1}^{N_{\mathrm{t}}} \frac{2N(j,\hat{\jmath})}{N_{\mathrm{t}}} P\left(\mathbf{x}_j \to \mathbf{x}_{\hat{\jmath}}\right), \end{aligned} \tag{4}$$

where $N(j,\hat{\jmath})$ is the number of bits in error between $\mathbf{x}_j$ and $\mathbf{x}_{\hat{\jmath}}$, $P\left(\mathbf{x}_j \to \mathbf{x}_{\hat{\jmath}}\right)$ denotes the pairwise error probability (PEP) of deciding on $\mathbf{x}_{\hat{\jmath}}$ given that $\mathbf{x}_j$ is transmitted, and where the index in the summation is simplified since $N\left(j,\hat{\jmath}\right)$ is symmetric. Using (1), we obtain the PEP conditioned on $\mathbf{H}$ as

$$\begin{aligned} P\left(\mathbf{x}_j \to \mathbf{x}_{\hat{\jmath}} \mid \mathbf{H}\right) &= P\left(d_{\hat{\jmath}} > d_j \mid \mathbf{H}\right) \\ &= P\left(\begin{array}{c} \mathrm{Re}\left\{\eta^H\left(\mathbf{h}_{\hat{\jmath}} - \mathbf{h}_j\right)\right\} \\ > \frac{\sqrt{\rho}}{2}\left\|\mathbf{h}_j - \mathbf{h}_{\hat{\jmath}}\right\|_{\mathrm{F}}^2 \mid \mathbf{H} \end{array}\right) \\ &= Q\left(\sqrt{\kappa}\right), \end{aligned}$$

where $d_j = \mathrm{Re}\left\{\left(\mathbf{y} - \frac{\sqrt{\rho}}{2}\mathbf{h}_j\right)^H \mathbf{h}_j\right\}$, and $Q(x) = \int_x^\infty \frac{1}{2\pi} e^{-\frac{t^2}{2}} dt$. We define κ as

$$\kappa \triangleq \frac{\rho}{2}\left\|\mathbf{h}_j - \mathbf{h}_{\hat{\jmath}}\right\|_{\mathrm{F}}^2 = \sum_{n=1}^{2N_{\mathrm{r}}} \alpha_n^2, \tag{5}$$

where $\alpha_n \sim \mathcal{N}\left(0, \sigma_\alpha^2\right)$ with $\sigma_\alpha^2 = \frac{\rho}{2}$. Note that the metric affecting the system performance is the Euclidean distance between the columns of $\mathbf{H}$.

The random variable κ in (5) is chi-squared distributed with $s = 2N_{\mathrm{r}}$ degrees of freedom, and PDF given by [24, p. 41] $p_\kappa(v) = \frac{v^{\frac{s}{2}-1}\exp\left(-\frac{v}{2\sigma_\alpha^2}\right)}{\left(2\sigma_\alpha^2\right)^{\frac{s}{2}}\Gamma\left(\frac{s}{2}\right)}$, $v > 0$. The PEP can then be formulated as

$$\begin{aligned} P\left(\mathbf{x}_j \to \mathbf{x}_{\hat{\jmath}}\right) &= E_\kappa\left[P\left(\mathbf{x}_j \to \mathbf{x}_{\hat{\jmath}} \mid \mathbf{H}\right)\right] \\ &= \int_{v=0}^{\infty} Q\left(\sqrt{v}\right) p_\kappa(v)\, dv, \end{aligned} \tag{6}$$

which has a closed form expression given in [25, Eq. (64)]. Thus,

$$P\left(\mathbf{x}_j \to \mathbf{x}_{\hat{\jmath}}\right) = \gamma_\alpha^{N_{\mathrm{r}}} \sum_{k=0}^{N_{\mathrm{r}}-1} \binom{N_{\mathrm{r}}-1+k}{k} \left[1-\gamma_\alpha\right]^k, \tag{7}$$

where $\gamma_\alpha \triangleq \frac{1}{2}\left(1 - \sqrt{\frac{\sigma_\alpha^2}{1+\sigma_\alpha^2}}\right)$. Plugging (7) into (4), we obtain

$$P_{\mathrm{e,bit}}^{\mathrm{SSK}} \leq \frac{N_\Sigma \gamma_\alpha^{N_{\mathrm{r}}}}{N_{\mathrm{t}}} \sum_{k=0}^{N_{\mathrm{r}}-1} \binom{N_{\mathrm{r}}-1+k}{k} \left[1-\gamma_\alpha\right]^k, \tag{8}$$

where $N_\Sigma = \sum_{j=1}^{N_{\mathrm{t}}}\sum_{\hat{\jmath}=j+1}^{N_{\mathrm{t}}} 2N(j,\hat{\jmath})$.

As we will see in Section V-A, the bound in (8) is somewhat loose (~1 dB offset for $M = 8$), but captures the diversity of the system. The bound can be tightened further by considering only the number of nearest neighbors n_{neigh} in SSK's effective constellation space $\mathcal{X}^{\mathrm{eff}}$, and is given by

$$P_{\mathrm{e,bit}}^{\mathrm{SSK}} \leq n_{\mathrm{neigh}} N_{\mathrm{avg}} \gamma_\alpha^{N_{\mathrm{r}}} \sum_{k=0}^{N_{\mathrm{r}}-1} \binom{N_{\mathrm{r}}-1+k}{k} \left[1-\gamma_\alpha\right]^k, \tag{9}$$

where $N_{\mathrm{avg}} = \frac{N_\Sigma}{N_{\mathrm{t}}(N_{\mathrm{t}}-1)}$ represents the average $N\left(j,\hat{\jmath}\right)$. Since the effective constellation points $\mathbf{x}_{j,\mathrm{eff}}$ are random, n_{neigh} is a random variable, and depends on M.[5] For example, we will see from Section V-A that for $M = 8$, $n_{\mathrm{neigh}} \approx 2$.

[5]The randomness of $\mathbf{x}_{j,\mathrm{eff}}$ results in a random, non-symmetric n_{neigh} distribution. Hence, it is difficult to obtain a value for n_{neigh} (as opposed to symmetric distributions, which have fixed nearest neighbors).

B. Diversity

The expression in (8) does not explicitly indicate the diversity achieved by SSK. In order to clearly show the system diversity, we re-derive the error probability with a loose upper bound. Specifically, we use $Q(x) \leq \frac{1}{2}\exp\left(-\frac{x^2}{2}\right)$ [24, p. 54], and upper bound (6) by

$$\begin{aligned} P(\mathbf{x}_j \to \mathbf{x}_{\hat{j}}) &\leq \int_0^{\infty} \frac{\exp\left(-\frac{v}{2}\right) v^{N_\mathrm{r}-1} \exp\left(-\frac{v}{\rho}\right)}{2\rho^{N_\mathrm{r}}\Gamma(N_\mathrm{r})} dv \\ &= \frac{1}{2}\left(\frac{2}{\rho+2}\right)^{N_\mathrm{r}} \leq 2^{N_\mathrm{r}-1}\rho^{-N_\mathrm{r}}. \end{aligned}$$

Therefore, the bit error probability is given by

$$P_{\text{e,bit}}^{\text{SSK}} \leq C\rho^{-N_\mathrm{r}}, \tag{10}$$

where $C = \frac{N(j,\hat{j})2^{N_\mathrm{r}-1}}{N_\mathrm{t}}$. We see from (10) that a diversity order of N_r is achieved, which is identical to an APM-MRC system using N_r receive antennas.

C. Complexity

In this part, we compare SSK's complexity to that of SM-OD. Since SM-OD is shown to exhibit similar complexity to that of SM [19], the reader is referred to [13] for other complexity comparisons (e.g., V-BLAST).

In our presentation, we quantify complexity by the number of multiplications required in the detection process. The number of additions can be shown to have a similar value for both detectors. In [19], the complexity of SM-OD is given by $\delta_{\text{SM-OD}} = 2N_\mathrm{r}N_\mathrm{t} + N_\mathrm{t}M + M$. Similar to [13], we analyze (1) to obtain SSK's complexity, which is given by

$$\delta_{\text{SSK}} = N_\mathrm{r}M.$$

It is important to note that, for the same spectral efficiency, the value of N_t and M for SM-OD and SSK are different. For SM-OD, M denotes the constellation size of the APM scheme. The total constellation size of SM-OD is MN_t. At first glance, it is not straightforward to compare both detector complexities. However, for practical values of N_t, N_r, and M, SSK can be shown to have lower complexity. For example, let us fix $m = 3$ bits/s/Hz transmission ($N_\mathrm{r} = 2$), and use $N_\mathrm{t} = 4$ and $M = 2$ for SM-OD. We then obtain $\delta_{\text{SSK}} = 16$, and $\delta_{\text{SM-OD}} = 26$. In this case, SM-OD requires more than 50% complex multiplications.

IV. SSK Coded Modulation

CM techniques have been extensively considered in the communications literature, with one of the most significant contributions stemming from Ungerboeck's seminal paper on trellis CM (TCM) [26], where coding and modulation are optimized as a single unit. As an enhancement, turbo CM (TuCM) [27]–[31] provides performance improvements over TCM by incorporating the turbo principle (turbo codes with iterative decoding). In [32], Zehavi improves TCM's performance in Rayleigh fading channels by separating coding and modulation with a bit-wise interleaver. Caire et al. [33] then extend Zehavi's concept to general constellations, giving rise to BICM systems, which are shown to provide higher diversity gains over conventional TCM systems. In this section, we focus on BICM systems due to these performance advantages, and inherent flexibility of analysis in varying scenarios.

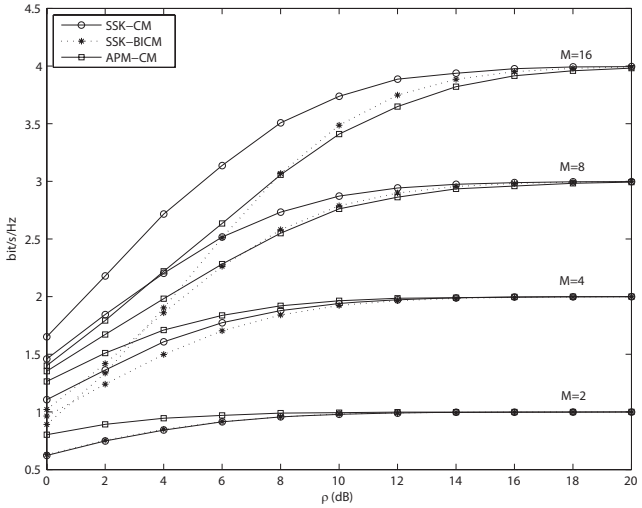

Fig. 3. SSK constrained input capacity versus SNR, for varying M ($N_\mathrm{r} = 2$).

A. Capacity

The capacity of the SSK system is computed for flat Rayleigh fading channels. Assuming $\mathbf{x}$ is transmitted with equal probability (which is justified for an ideally interleaved sequence of channel inputs), the constrained input CM capacity reduces to [33]

$$C_{\text{CM}} = m - E_\theta\left[\log_2 \frac{\sum_{\mathbf{x}'\in\mathcal{X}} p_{\mathbf{Y}}(\mathbf{y}|\mathbf{x}',\mathbf{H})}{p_{\mathbf{Y}}(\mathbf{y}|\mathbf{x},\mathbf{H})}\right], \tag{11}$$

where $m = \log_2(N_\mathrm{t})$, $\theta = (\mathbf{x}, \mathbf{y}, \mathbf{H})$, and $p_{\mathbf{Y}}(\mathbf{y} \mid \mathbf{x}, \mathbf{H})$ is given in (2). The capacity results for SSK modulation with varying M (evaluated by Monte Carlo simulations) are shown in Fig. 3. We compare the capacity of systems requiring only one transmit antenna (similar to that of an SSK system) and hence, we plot the information rates of PSK for $M \leq 8$ and QAM for $M = 16$. SSK achieves better information rates when $M \geq 8$, and slightly worse for $M < 8$. These results are expected since, for small M values, APM schemes exploit enough of the constellation space to achieve adequate performance (Section II-C).

We also plot the BICM capacity (dotted lines), which represents the capacity between the encoder output and the input of the decoder. With some change of notation, the BICM capacity is given by [33]

$$C_{\text{BICM}} = m - \sum_{k=1}^{m} E_\theta\left[\log_2\left(\frac{\sum_{\mathbf{x}'\in\mathcal{X}} p_{\mathbf{Y}}(\mathbf{y}|\mathbf{x}',\mathbf{H})}{\sum_{\mathbf{x}'\in\mathcal{X}_c^k} p_{\mathbf{Y}}(\mathbf{y}|\mathbf{x}',\mathbf{H})}\right)\right].$$

For increasing M, SSK's BICM capacity degrades (especially at low SNRs), which is expected since symbol mappings are not optimized in the BICM system, as suggested by [33]–[35]. In fact, since SSK's effective constellation points are random in nature, optimal mapping techniques cannot be considered without sufficient channel state information (CSI)

at the transmitter. Regardless, the capacity results for CM still indicate SSK performance improvements over APM schemes.

In order to obtain more insight, and support our capacity results, we analytically derive the performance of SSK-CM in Section IV-D. But first, we describe the structure of the SSK-CM system, and the adopted decoding method.

B. Encoding

Conventional modulation schemes use Gray (or quasi-Gray) mapping to minimize bit errors amongst symbols. For the case of TCM, bits to symbol mapping is optimized so as to maximize the Euclidean distance between codewords. However, due to random constellation points inherent in SSK modulation, SSK-TCM is only possible when full channel knowledge is available at the transmitter. For that reason, capacity maximizing CM techniques cannot be considered in SSK. In our take on SSK-CM, we consider SSK-BICM without any optimized mapping rule, and opt for BICM with iterative decoding (BICM-ID) to bridge the capacity gaps observed in Fig. 3 (see [36] for details).

The encoding is described in Section II, where information bits are first encoded, bit-wise interleaved, and SSK modulated before transmission. Both TuCM and convolutional CM systems are considered, but there is no restriction on the type of channel code $\mathcal{C}$ used.

C. Decoding

SSK coded detection employs BICM-ID, and follows the decoding structure proposed by Li and Ritcey in [37], and is depicted in Fig. 1. The demodulator first computes the *a posteriori* logarithm likelihood ratios (LLR) of the transmitted bits, which are then used as inputs to a channel decoder. Depending on $\mathcal{C}$, we use either a turbo or a maximum *a posteriori* (MAP) decoder (see [38, Ch. 7] for details). The channel decoder's LLR on the information and parity bits are then processed as extrinsic information in successive iterations of the demodulator's LLR output (shown by the dashed lines in Fig. 1). These steps are repeated until a satisfactory level of reliability is obtained (for our case, we consider a fixed number of iterations).

The demodulator LLR, similar to [31], is given by

$$\begin{aligned}\Lambda_{\text{DEM}}(\hat{c}) &= \log\frac{P(\hat{c}=1\mid\mathbf{y})}{P(\hat{c}=0\mid\mathbf{y})}\\ &= \log\frac{\sum\limits_{\mathbf{x}\in\mathcal{X}_1^k} p_{\mathbf{Y}}(\mathbf{y}|\mathbf{x},\mathbf{H})\prod\limits_{n=1,n\neq k}^{m} P(c_n)}{\sum\limits_{\mathbf{x}\in\mathcal{X}_0^k} p_{\mathbf{Y}}(\mathbf{y}|\mathbf{x},\mathbf{H})\prod\limits_{n=1,n\neq k}^{m} P(c_n)},\end{aligned} \tag{12}$$

where $p_{\mathbf{Y}}(\mathbf{y}\mid\mathbf{x},\mathbf{H})$ is given by (2), and $P(c_n=c)=\frac{e^{c\Lambda_{\text{DEC}}(c_n)}}{1+e^{\Lambda_{\text{DEC}}(c_n)}}, c\in\{0,1\}$ is obtained from the LLR values of the decoder, $\Lambda_{\text{DEC}}(c_n)$. The same setup is employed for the APM-CM case.

D. Coded Error Probability

In this section, SSK-CM's analytical performance for fully interleaved channels (each symbol experiences an independent fading matrix) is derived. Thanks to the binary input-output symmetric (BIOS) property of BICM systems, the performance analysis is tractable.[6] We assume a convolutional coded system, concatenated with an SSK modulator, but can be generalized to other concatenated schemes as well (e.g., TuCM [39]).

The analysis for the coded case is fairly complex, especially due to interleaving and iterative decoding effects. The simplifying analysis performed in most coding literature regarding the all zero codeword is no longer valid due to the nonlinearity of CM systems. Therefore, similar to [39], all codeword pairs must be considered in order to obtain an analytical expression for the error probability. Most often, however, simple union bound on the BER is used. From [33], [40], the bit error probability for BICM under ML decoding is closely upper bounded by

$$P_{\text{e,bit}} \leq B(X)\big|_{X=[\text{PEP}(d,\mu,\mathcal{X},\rho)]^{\frac{1}{d}}}, \tag{13}$$

where $B(X)\triangleq\sum B_d X^d$, $B_d=\sum_i \frac{i}{k}A_{i,d}$ ($A_{i,d}$ represents the number of codewords in $\mathcal{C}$ with output Hamming weight d and input weight i), μ is the labeling rule for the constellation $\mathcal{X}$, and ρ is the SNR at each receive antenna.

In order to further simplify the analysis, we incorporate the LLR within the derivation as in [33]. Therefore, the statistical properties of the LLR random variable are required. Specifically, we need a closed form expression for the PDF of the LLR, $p_\Lambda(\lambda)$. These PDFs are obtained in [41] for APM, but difficult to derive in the case of multi-dimensional constellations. To overcome this challenge, [42] presents simple upper bounds based on saddlepoint (SP) approximations, without explicitly determining $p_\Lambda(\lambda)$. The BICM PEP is then upper bounded using SP approximations (for fully interleaved channels) as [42]

$$\text{PEP}_{\text{BICM}}(d,\mu,\mathcal{X},\rho)\approx\frac{\exp(d\tau(\hat{s}))}{\sqrt{2\pi d\tau''(\hat{s})}\hat{s}}, \tag{14}$$

where $\tau(\hat{s})$ is the cumulant generating function of the random variable Λ_{DEM} defined in (12), $\tau''(\hat{s})$ represents its second derivative, and with $\hat{s}=\frac{1}{2}$ for BIOS channels. Equation (14) is plugged into (13) to obtain an upper bound on $P_{\text{e,bit}}$, which is conveniently evaluated by Monte Carlo simulations, or by using numerical integration methods with Gaussian quadrature rules (see [42] for details).

Equation (14) does not take into consideration the effects of iterative decoding, which is the type of decoder employed in this paper. Hence, (14) is strictly an upper bound for the BICM-ID case. In order to make fair comparisons, asymptotic BICM-ID bounds are derived, and valid after convergence (i.e., for sufficiently high SNRs and large number of decoding iterations). These bounds are also referred to as the error-free feedback performance [43]. An error-free feedback assumption implies that each bit is transmitted using an equivalent BPSK type system. Consequently, we are able to directly use the results of [44], and obtain closed form PEP bounds on error-free feedback. Noting that for SSK, $\Lambda_{\text{DEM}}\sim\mathcal{N}\left(-4N_{\text{r}}^{-1}\kappa, 8N_{\text{r}}^{-1}\kappa\right)$, where $\kappa=\frac{\rho}{2}\|\mathbf{h}_j-\mathbf{h}_{\hat{j}}\|_{\text{F}}^2$ represents the effective SNR, we obtain the saddlepoint approximation

[6]For signal constellations $\mathcal{X}$ leading to a non-symmetric BICM channel, a method to symmetrize the channel is presented in [33].

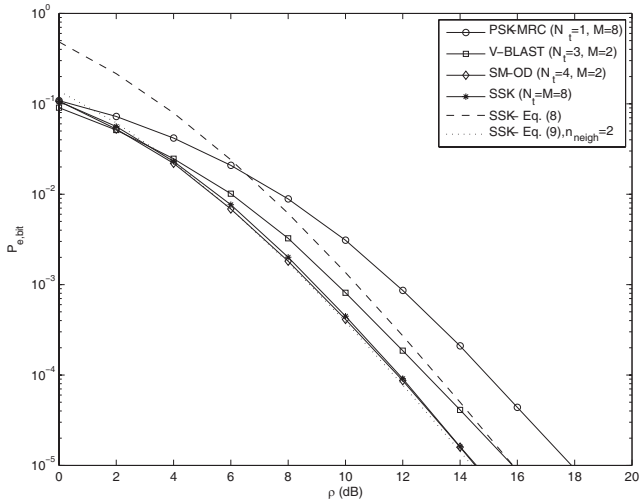

Fig. 4. BER performance of SSK versus MRC, V-BLAST, and SM, for $m = 3$ bits/s/Hz transmission ($N_\mathrm{r} = 4$).

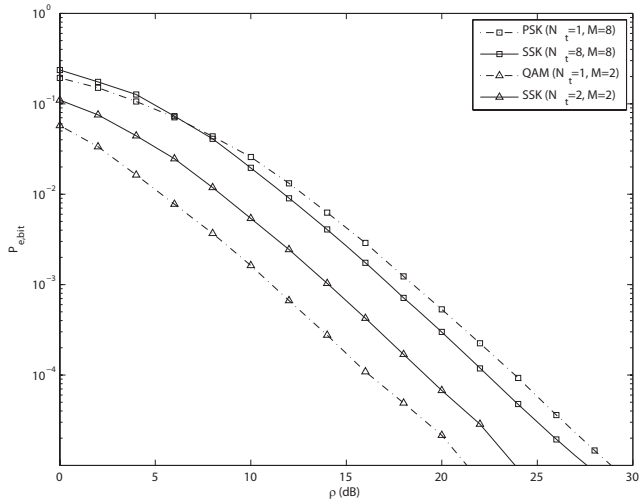

Fig. 5. BER performance of SSK versus MRC, for varying M ($N_\mathrm{r} = 2$).

for the PEP as [44, Eq. (28)]

$$\mathrm{PEP}_{\text{BICM-ID}}\left(d, \mu, \mathcal{X}, \rho\right) \approx \frac{1}{2\sqrt{\pi d \rho}} \left(1 + \frac{\rho}{N_\mathrm{r}}\right)^{-dN_\mathrm{r}+\frac{1}{2}}. \quad (15)$$

Remark 2: The error-free feedback bounds for SSK are independent of the constellation size. Hence, SSK-CM's asymptotic performance is identical for all M. This is not the case for APM-CM, where the performance degrades as M is increased. This degradation is due to the decrease in average Euclidean distance between equivalent BPSK symbols (obtained from the constellation of size M). However, the equivalent BPSK symbols in SSK will have (on average) the same Euclidean distance regardless of M.

V. Simulation Results

In this section, some examples are presented to compare SSK's performance for varying parameters (such as M and N_r). Monte Carlo simulations are performed, and are run for at least 10^5 channel realizations. All results consider a Rayleigh fading channel (described in Section II), with complete channel knowledge at the receiver. We also use Gray (or quasi-Gray) mapping when appropriate (i.e., for PSK and QAM). The plots illustrate the average BER performance versus ρ (the average SNR per receive antenna).

A. SSK versus SM, MRC and V-BLAST

Figure 4 demonstrates SSK's performance versus MRC, V-BLAST, and SM. We target $m = 3$ bits/s/Hz transmission, with $N_\mathrm{r} = 4$. For reference, three different transmission setups are used. The first one is APM, 8-PSK transmission with $N_\mathrm{t} = 1$, and MRC. The second is V-BLAST with BPSK modulation, $N_\mathrm{t} = 3$, and ordered successive interference cancellation (OSIC) using the minimum mean squared error (MMSE) receiver [2]. Finally, the third setup is SM-OD [19], where we use $N_\mathrm{t} = 4$ antennas, and BPSK modulation (which results in $N_\mathrm{t} \cdot M = 8$ constellation points).

The bounds of (8) are also plotted for comparison, where $N_\mathrm{t} = 8$, $\sigma_\alpha^2 = \frac{\rho}{2}$, and $N_\Sigma = 96$. We also tighten the bound by considering a heuristic number of nearest neighbors (as discussed in Section III-A). We plot (9) with $n_{\text{neigh}} = 2$, where the value for n_{neigh} is obtained by trial and error, and we observe that both bounds are fairly tight, especially at high SNRs.

SSK's performance improvements is clearly shown in Fig. 4, where we observe gains of 3 dB over APM and 1 dB over V-BLAST (at $P_{\text{e,bit}} = 10^{-5}$). SSK has almost identical performance to that of SM-OD, but with lower complexity (attributed to the fact that symbols do not carry information such as in SM and APM-MRC).

We note that the comparison between V-BLAST and SSK is under the assumption of identical transmission rate. However, V-BLAST can be designed with varying number of antennas and modulation sizes to achieve the desired rate. Our example uses only one of these combinations for illustration purposes. Conclusive remarks cannot be made on which system performs better, due to the additional hardware requirements needed to support larger number of antennas for V-BLAST, whereas much more relaxed for SSK (as mentioned in Section II). For this reason, we focus on systems with hardware needs resembling that of SSK (i.e., APM and SM).

B. SSK versus APM

In the next examples, we present comparisons of SSK to single antenna APM schemes.

1) Varying M: The effects of the constellation size M on performance is illustrated in Fig. **??**, where the BER performance of SSK and APM schemes for $M = 2$ and 8 are shown. In light of the discussion in Section II-C, we expect SSK to outperform APM for higher modulation order. With $M = 2$, APM outperforms SSK as expected, whereas with $M = 8$, it is SSK exhibiting better performance.

2) Varying N_r: Figure 6 illustrates the effect of varying N_r on SSK's performance. We target $m = 3$ bits/s/Hz, and hence consider 8-PSK and 8-SSK modulation. We notice that SSK's diversity order is identical to APM, as derived in Section III-B. However, SSK achieves SNR gains of about 4 dB over APM at $P_{\text{e,bit}} = 10^{-5}$ ($N_\mathrm{r} = 4$). Also, SSK gains more in terms of

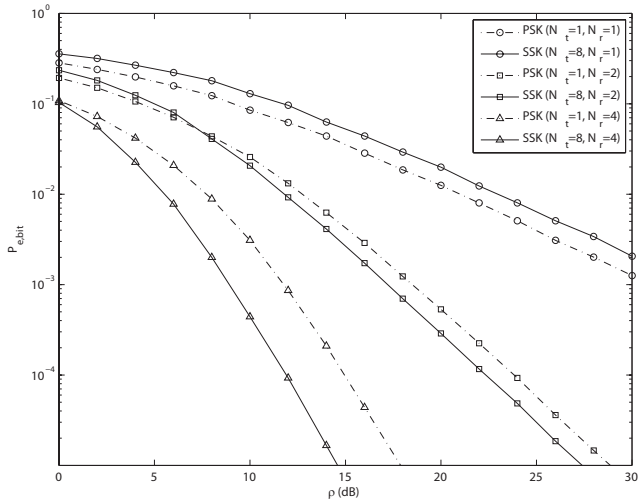

Fig. 6. BER performance of SSK versus MRC, for varying N_{r} ($M = 8$).

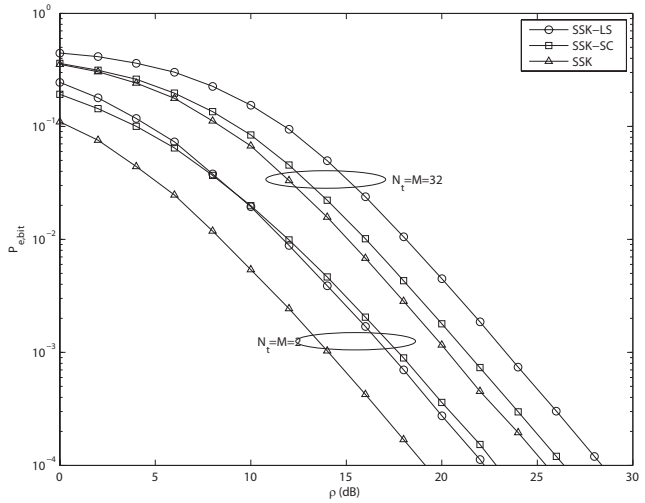

Fig. 7. BER performance of SSK under non-ideal conditions, for varying M ($N_{\mathrm{r}} = 2$).

performance as N_{r} is varied compared to APM. For example, for $N_{\mathrm{r}} = 2$ to $N_{\mathrm{r}} = 4$, SSK gains 12 dB whereas PSK only gains about 10 dB.

C. SSK under non-ideal conditions

In this example, the effect of certain real-world non-idealities on the performance of SSK is studied. In particular, we consider CSI estimation effects and spatial correlation (SC) amongst antennas.

CSI estimation: Estimation of the channel matrix $\mathbf{H}$ is performed using pilot symbols for least square (LS) estimation [45]. The estimated channel matrix $\hat{\mathbf{H}}_{\mathrm{LS}}$ is given by $\hat{\mathbf{H}}_{\mathrm{LS}} = \frac{1}{\sqrt{\rho}}\mathbf{y}_{\mathrm{p}}\mathbf{x}_{\mathrm{p}}^{H}\left(\mathbf{x}_{\mathrm{p}}\mathbf{x}_{\mathrm{p}}^{H}\right)^{-1}$, where the subscript "p" is used to indicate that the input and output are obtained using pilot symbols. In [46], it is shown that $\mathbf{x}_{\mathrm{p}}$ using constant energy orthogonal rows make for optimal pilot symbols. Therefore, we use $\mathbf{x}_{\mathrm{p}} = \mathbf{I}_{N_{\mathrm{t}}}$, which is essentially a symbol set taken form SSK modulation. With such inputs, the LS solution becomes $\hat{\mathbf{H}}_{\mathrm{LS}} = \mathbf{H} + \frac{\eta}{\sqrt{\rho}}$. Therefore, the effect of estimation error is simply a shift in SSK's performance, attributed to the fact that the estimated channel is now distributed according to $\mathcal{CN}\left(0, \frac{1+\rho}{\rho}\right)$.

Although SSK detection assumes perfect channel estimation, the decoder will still function with imperfect channel estimates (as we will see in Fig. 7). This is because, even in the low SNR region, where channel estimates are less accurate, it is not the actual channel realizations that drives performance, but rather the distance between the columns of $\mathbf{H}$. Hence, detection is still possible (where the estimation errors only contribute to additive noise).

Spatial Correlation: Assuming the presence of local scatters around both transmitter and receiver, one widely accepted model for spatial correlation (SC) is given in [47] as $\mathbf{H}_{\mathrm{corr}} = \mathbf{R}_{\mathrm{r}}^{\frac{1}{2}}\mathbf{H}\mathbf{R}_{\mathrm{t}}^{\frac{1}{2}}$, where $\mathbf{R}^{\frac{1}{2}}$ represents the matrix square root (i.e., $\mathbf{R}^{\frac{1}{2}}\mathbf{R}^{\frac{1}{2}} = \mathbf{R}$). In our presentation of SC, we obtain the correlation matrices according to [48]

$$\mathbf{R}(r,c) = \mathbf{R}^{*}(c,r) = \rho_{\mathrm{corr}}^{r-c}, \quad r \geq c \ , \tag{16}$$

where $\mathbf{R}(r,c)$ represents the element of $\mathbf{R}$ in the r^{th} row and c^{th} column, and ρ_{corr} represents the amount of correlation ($|\rho_{\mathrm{corr}}| < 1$). Equation (16) may not be an accurate method for generating the correlation coefficients in real world scenarios. However, this simple parameter model gives us quick insight into the effects of SC on SSK modulation. Note that the model does follow some reasonable physical characteristics, such as the decrease in correlation with the increase between antenna distance. More realistic correlation matrices can be obtained given specific channel scenarios (see [49], [50]), which vary according to the application.

Figure 7 illustrates SSK's performance under non-ideal scenarios, for varying modulation size M. As expected, the degradation in performance due to CSI estimation error (using LS) is relatively the same for both M values (about 3 dB). With SC ($\rho_{\mathrm{corr}} = 0.5$) on the other hand, SSK experiences larger loss in performance for $M = 2$ than $M = 32$, which is expected. We know from Section II-C that for increasing M (with N_{r} fixed), SSK's constellation space becomes more crowded. Therefore, by introducing correlation in an already crowded space (i.e., $M = 32$), the performance is not degraded by much. However, for $M = 2$, the constellation points are widely spread apart, but adversely affected due to the correlation, and hence, more degradation is observed.

D. Coded SSK Modulation

In this section, we illustrate SSK's performance with coding. In particular, we present examples to compare SSK's performance using different parameters (such as M and the number of decoding iterations). The receiver is assumed to be the iterative demodulator-decoder from Fig. 1.

1) SSK-CM versus APM-CM (varying M): In this example, we consider a convolutional CM system using a rate $\frac{1}{2}$ convolutional encoder given by the generator matrix $G = \left[1 \quad \frac{1+D^2}{1+D+D^2}\right]$, with a block length of $L = 1000$.

Figure 8 illustrates SSK-CM's performance for $M = 8$ and $M = 16$. For fully interleaved channels, both SSK and APM have the same diversity advantage but with SSK still

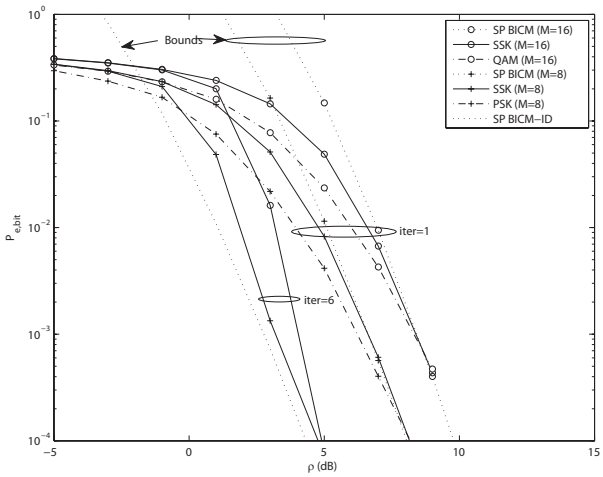

Fig. 8. BER performance of SSK-CM versus APM-CM, for vaying number of iterations and M ($N_{\mathrm{r}} = 2$) in fully interleaved channels.

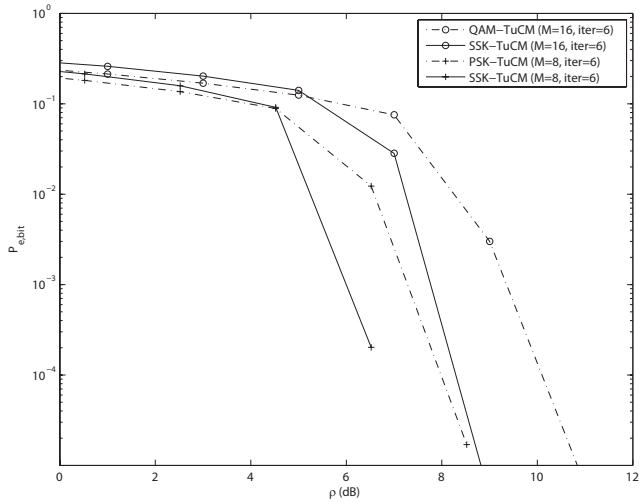

Fig. 9. BER performance of SSK-TuCM versus APM-TuCM for varying M ($N_{\mathrm{r}} = 2$) in fully interleaved channels.

outperforming APM (about 3 dB and 5 dB for $M = 8$ and 16, respectively, at $P_{\mathrm{e,bit}} = 10^{-4}$). We also plot SSK's SP bounds on BER, using the BICM PEP of (14), and the error-free feedback PEP of (15), with $B(X) = \frac{3X^5 - 6X^6 + 2X^7}{1 - 4X + 4X^2}$ [40, p. 504]. To validate the obtained bounds, we simulate SSK-CM for one decoding iteration (i.e., BICM without ID), and six decoding iterations (i.e., asymptotic BICM-ID). We observe that the BICM bounds are fairly tight, especially at high SNRs, while the error-free feedback bounds denote a lower limit on SSK-BICM-ID's performance. APM-CM results are only shown for two iterations, since theoretically, iterative demodulation-decoding of a gray-mapped APM system does not improve much on performance (see APM capacity results of BICM versus CM in [33, Fig. 5]).

2) SSK-TuCM versus APM-TuCM (varying M): In this example, we obtain performance results for higher coding rates. We use a rate $\frac{3}{4}$ punctured turbo code composed of two, rate $\frac{1}{2}$ convolutional encoders given by the generator matrix $G = \left[1 \quad \frac{1+D+D^2+D^3}{1+D^2+D^3}\right]$ ($L = 1000$), where we consider one turbo decoding iterations for each demodulator-decoder iteration.

Figure 9 illustrates SSK-TuCM's performance for $M = 8$ and $M = 16$, respectively. SSK is shown to outperform APM by 1.5 dB and 2 dB for $M = 8$ and 16, respectively (for six demodulator-decoder iterations, and $P_{\mathrm{e,bit}} = 10^{-4}$). As well, the results are relatively close to capacity. For example, the results for 8-SSK tend to $P_{\mathrm{e,bit}} = 10^{-5}$ at about 7 dB, which is 2 dB away from capacity (i.e., $\frac{9}{4}$ bit/s/Hz is achieved at around 5 dB, c.f. Fig. 3). For 16-SSK, the results tend to $P_{\mathrm{e,bit}} = 10^{5}$ at about 8.5 dB, which is about 3 dB away from capacity.

VI. Conclusion

In this paper, we introduced a modulation technique (referred to as SSK) for MIMO wireless links. We laid out SSK fundamentals as the building ground for hybrid modulation schemes (i.e., combination of SSK and APM such as in [6], [14], [16], [20]), while also providing closed form upper bounds on the bit error probability. We also presented coded SSK, which was shown to achieve higher capacity results than APM. We derived closed form upper bounds on the bit error probability of the coded system, and showed performance gains over APM (for convolutional and turbo codes). All of SM's merits mentioned in [20] are *also* inherent in SSK, but with lower computational overhead and with relaxed APM hardware requirements. These advantages make SSK a promising candidate for low complexity transceivers in next generation communication systems. Future research directions will involve hybrid SSK systems combining popular MIMO architectures, and practical SSK implementation issues in current MIMO communication standards (such as UWB).

References

[1] P. Wolniansky, G. Foschini, G. Golden, and R. Valenzuela, "V-BLAST: an architecture for realizing very high data rates over the rich-scattering wireless channel," in *Proc. International Symp. Signals, Systems, Electronics (ISSSE'98)*, Pisa, Italy, pp. 295-300, Sept. 1998.

[2] R. Böhnke, D. Wübben, V. Kühn, and K. D. Kammeyer, "Reduced complexity MMSE detection for BLAST architectures," in *Proc. IEEE Globecom'03*, San Francisco, CA, USA, Dec. 2003.

[3] S. M. Alamouti, "A simple transmit diversity technique for wireless communications," *IEEE J. Select. Areas Commun.*, vol. 16, no. 8, pp. 1451-1458, Oct. 1998.

[4] V. Tarokh, H. Jafarkhani, and A. R. Calderbank, "Space-time block code from orthogonal designs," *IEEE Trans. Inform. Theory*, vol. 45, pp. 1456-1467, July 1999.

[5] V. Tarokh, A. Naguib, N. Seshadri, and A. R. Calderbank, "Combined array processing and space-time coding," *IEEE Trans. Inform. Theory*, vol. 45, pp. 1121-1128, May 1999.

[6] R. Mesleh, H. Haas, Y. Lee, and S. Yun, "Interchannel interference avoidance in mimo transmission by exploiting spatial information," in *Proc. PIMRC'05*, Sept. 2005.

[7] Agilent Technologies, "E4438C-419 Signal Studio for 3GPP W-CDMA HSPA Online Documentation," [Online]. Available: http://wireless.agilent.com /wireless/helpfiles/opt419/opt419.htm#transmit_diversity.htm.

[8] A. F. Molisch and M. Z. Win, "MIMO systems with antenna selection," *IEEE Microw. Mag.*, vol. 5, no. 1, pp. 46-56, Mar. 2004.

[9] R. Heath and A. Paulraj, "Antenna selection for spatial multiplexing systems based on minimum error rate," in *Proc. IEEE Int. Contr. Conf.*, vol. 7, Helsinki, Finland, June 2001, pp. 2276-2280.

[10] R. W. Heath, Jr., S. Sandhu, and A. Paulraj, "Antenna selection for spatial multiplexing with linear receivers," *IEEE Commun. Lett.*, vol. 5, no. 4, pp. 142-144, Apr. 2001.

[11] A. Ghrayeb and T. M. Duman, "Performance analysis of MIMO systems with antenna selection over quasi-static fading channels," *IEEE Trans. Veh. Technol.*, vol. 52, pp. 281-288, Mar. 2003.
[12] R. W. Heath, Jr and D. J. Love, "Multimode antenna selection for spatial multiplexing systems with linear receivers," *IEEE Trans. Signal Processing*, vol. 53, no. 8, pp. 3042-3056, Aug. 2005.
[13] R. Mesleh, H. Haas, C. Ahn, and S. Yun, "Spatial modulation—a new low complexity spectral efficiency enhancing technique," in *Proc. First international Conf. Commun. Networking China (ChinaCom'06)*, pp. 1-5, Oct. 2006.
[14] Y. A. Chau and S.-H. Yu, "Space modulation on wireless fading channels," in *Proc. IEEE 54th VTC' 01 (Fall)*, vol. 3, pp. 1668-1671, 2001.
[15] Y. A. Chau and S.-H. Yu, "Space shift keying modulation," US Patent Application Publication, # 0094783, July 2002.
[16] H. Haas, E. Costa, and E. Schulz, "Increasing spectral efficiency by data multiplexing using antenna arrays," in *Proc. PIMRC'02*, vol. 2, pp. 610-613, Sept. 15-18, 2002.
[17] R. Mesleh, H. Haas, C. W. Ahn, and S. Yun, "Spatial modulation-OFDM," in *Proc. 11th International OFDM-Workshop 2006 (InOWo'06)*, pp. 288-292, Aug. 2006.
[18] S. Ganesan, R. Mesleh, H. Haas, C. W. Ahn, and S. Yun, "On the performance of spatial modulation OFDM," in *Proc. 40th Asilomar Conf. Signals, Systems Computers*, pp. 1825-1829, Oct. 2006.
[19] J. Jeganathan, A. Ghrayeb, and L. Szczecinski, "Spatial modulation: optimal detection and performance analysis," *IEEE Commun. Lett.*, vol. 12, no. 8, pp. 545-547, Aug. 2008.
[20] R. Mesleh, H. Haas, S. Sinanović, C. W. Ahn, and S. Yun, "Spatial modulation," *IEEE Trans. Veh. Technol.*, vol. 57, no. 4, pp. 2228-2241, July 2008.
[21] A. F. Molisch *et al.*, "A comprehensive standardized model for ultrawideband propagation channels," *IEEE Trans. Antennas Propag.*, vol. 54, no. 11, pp. 3151-3166, Nov. 2006.
[22] J. Jeganathan, "Space shift keying modulation for MIMO channels," M.A.Sc. thesis, Concordia University, Montreal, QC, Aug. 2008.
[23] J. Jeganathan, A. Ghrayeb, and L. Szczecinski, "Generalized space shift keying modulation for MIMO channels," *IEEE International Symposium Personal, Indoor Mobile Radio Commun. (PIMRC'08)*, Cannes, France, Sept. 2008.
[24] J. G. Proakis, *Digital Communications*, (4th ed.) New York: McGraw-Hill, 2001.
[25] M.-S. Alouini and A. Goldsmith, "A unified approach for calculating error rates of linearly modulated signals over generalized fading channels," *IEEE Trans. Commun.*, vol. 47, no. 9, pp. 1324-1334, Sept. 1999.
[26] G. Ungerboeck, "Channel coding with multilevel/phase signals", *IEEE Trans. Inform. Theory*, vol. 28, no. 1, pp. 55-67, Jan. 1982.
[27] S. Le Goff, A. Glavieux, and C. Berrou, "Turbo-codes and high spectral efficiency modulation," in *Proc. IEEE Int. Conf. Commun.*, 1994, pp. 645-649.
[28] P. Robertson and T. Woerz, "Novel bandwidth efficient coding scheme employing turbo codes," in *Proc. IEEE Int. Conf. Commun.*, 1996, pp. 962-967.
[29] S. Benedetto, D. Divsalar, G. Montorsi, and F. Pollara, "Parallel concatenated trellis-coded modulation," in *Proc. IEEE Int. Conf. Commun.*, 1996, pp. 974-978.
[30] T. M. Duman, "Turbo codes and turbo coded modulation systems: analysis and performance bounds," Ph.D. dissertation, Northeastern University, Dept. of Electrical and Computer Engineering, Boston, MA, 1998.
[31] A. Stefanov and T.M. Duman, "Turbo-coded modulation for systems with transmit and receive antenna diversity over quasi-static fading channels: system model, decoding approaches, and practical considerations," *IEEE J. Select. Areas Commun.*, vol. 19, no. 5, pp. 958-968, May 2001.
[32] E. Zehavi, "8-PSK trellis codes for a Rayleigh channel," *IEEE Trans. Commun.*, vol. 40, pp. 873-884, May 1992.
[33] G. Caire, G. Taricco, and E. Biglieri, "Bit-interleaved coded modulation," *IEEE Trans. Inform. Theory*, vol. 44, pp. 927-947, May 1998.
[34] S. Y. Le Goff, "Signal constellations for bit-interleaved coded modulation," *IEEE Trans. Inform. Theory*, vol. 49, pp. 307-313, Jan. 2003.
[35] N. H. Tran and H. H. Nguyen, "Design and performance of BICM-ID systems with hypercube constellations," *IEEE Trans. Wireless Commun.*, vol. 5, no. 5, pp. 1169-1179, May 2006.
[36] F. Schreckenbach and G. Bauch, "Bit-interleaved coded irregular modulation," *Euro. Trans. Telecommun.*, vol. 17, no. 2, pp. 269–282, Mar.-Apr. 2006.
[37] X. Li and J. A. Ritcey, "Bit-interleaved coded modulation with iterative decoding," in *Proc. IEEE Int. Conf. Commun. (ICC'99)*, June 1999, pp. 858-862.
[38] T. M. Duman and A. Ghrayeb, *Coding for MIMO Communication Systems*. Wiley, 2007.
[39] T. M. Duman and M. Salehi, "Performance bounds for turbo-coded modulation systems," *IEEE Trans. Commun.*, vol. 47, pp. 511-521, Apr. 1999.
[40] S. Lin and D. J. Costello, Jr., *Error Control Coding*, (2nd ed.) Upper Saddle River, NJ: Pearson Prentice Hall, 2004.
[41] L. Szczecinski, R. Bettancourt, and R. Feick, "Probability density function of reliability metrics in BICM with arbitrary modulation: closed-form through algorithmic approach," *IEEE Trans. Commun.*, vol. 56, no. 5, pp. 736-742, May 2008.
[42] A. Martinez, A. Guillén i Fàbregas, and G. Caire, "Error probability of bit-interleaved coded modulation," *IEEE Trans. Inform. Theory*, vol. 52, no. 1, pp. 262-271, Jan. 2006.
[43] A. Chindapol and J. A. Ritcey, "Design, analysis and performance evaluation for BICM-ID with square QAM constellations in Rayleigh fading channels," *IEEE J. Select. Areas Commun.*, vol. 19, pp. 944-957, May 2001.
[44] A. Martinez, A. Guillén i Fàbregas, and G. Caire, "A closed-form approximation for the error probability of BPSK fading channels," *IEEE Trans. Wireless Commun.*, vol. 6, no. 6, pp. 2051-2054, June 2007.
[45] S. Kay, *Fundamental of Statistical Signal Processing: Estimation Theory*, vol. 1. Prentice Hall, 1993.
[46] M. Biguesh and A. B. Gershman, "MIMO channel estimation: optimal training and tradeoffs between estimation techniques," in *Proc. ICC*, Paris, France, June 2004, vol. 5, pp. 2658-2662.
[47] D. Shiu, G. Foschini, M. Gans, and J. Kahn "Fading correlation and its effect on the capacity of multi-element antenna systems," *IEEE Trans. Commun.*, vol. 48, no. 3, pp. 102-513, Mar. 2000.
[48] S. L. Loyka, "Channel capacity of MIMO architecture using the exponential correlation matrix," *IEEE Commun. Lett.*, vol. 5, pp. 369-371, Sept. 2001.
[49] A. Forenza, D. J. Love, and R. W. Heath, Jr., "A low complexity algorithm to simulate the spatial covariance matrix for clustered MIMO channel models," in *Proc. IEEE Veh. Technol. Conf.*, May 2004, vol. 2, pp. 889-893.
[50] K. I. Pedersen, P. E. Mogensen, and B. H. Fleury, "A stochastic model of the temporal and azimuthal dispersion seen at the base station in outdoor propagation environments," *IEEE Trans. Veh. Technol.*, vol. 49, pp. 437-447, Mar. 2000.

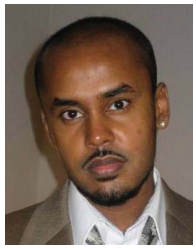

Jeyadeepan Jeganathan received the B.Eng. (with great distinction) and M.A.Sc. degrees from Concordia University, Montreal, QC, Canada, in 2006 and 2008, respectively, all in electrical engineering.

He is now a system integrator at Ericsson, Montreal, QC, Canada for their mobile soft switch solution. His current research interests are in wireless networking and long term evolution (LTE) systems.

Ali Ghrayeb (S'97,M'00,SM'06) received the Ph.D. degree in electrical engineering from the University of Arizona, Tucson, in 2000. He is currently an Associate Professor with the Department of Electrical and Computer Engineering, Concordia University,Montreal, QC, Canada. He holds a Concordia University Research Chair in High-Speed Wireless Communications. He is the coauthor of the book Coding for MIMO Communication Systems (Wiley, 2008). His research interests include wireless and mobile communications, error correcting coding, MIMO systems, wireless cooperative networks, and CDMA/WCDMA systems.

Dr. Ghrayeb has co-instructed technical tutorials on Coding for MIMO Systems and on Synchronization for WCDMA Systems at several major IEEE conferences, including the Global Telecommunications Conference and the International Conference on Communications. He serves as an Associate Editor of the IEEE TRANSACTIONS ON VEHICULAR TECHNOLOGY. He served as an Associate Editor of the Wiley Wireless Communications and Mobile Computing Journal from 2004-2008.

Leszek Szczecinski (M'98-SM'07), received M.Eng. degree from the Technical. University of Warsaw in 1992, and Ph.D. from INRS-Telecommunications, Montreal, Canada in 1997. From 1998 to 2000, he was Assistant Professor at the Department of Electrical Engineering, University of Chile. Since 2001 he had been Assistant Professor, and since 2007, Associate Professor at INRS-EMT, Montreal, Canada. His research interests are in the area of digital signal processing, communication theory, wireless communications, and analysis and design of iterative (turbo) processing algorithms.

Andres Ceron was born in 1984 in Purranque, Chile. He received the M.Sc. degree in Electronic Engineering at Universidad Técnica Federico Santa María,Valparaíso, Chile in 2008. In 2007-2008 he was conducting research in the area of iterative receivers in collaboration with the Institut National de la Recherche Scientifique, Montreal, QC, Canada. His current research interests are wireless and mobile communications, advanced coding techniques, iterative processing, and data communications and networking.